



Article

Flood Management, Characterization and Vulnerability Analysis Using an Integrated RS-GIS and 2D Hydrodynamic Modelling Approach: The Case of Deg Nullah, Pakistan

Ijaz Ahmad ¹, Xiuquan Wang ^{2,*}, Muhammad Waseem ¹, Muhammad Zaman ³, Farhan Aziz ², Rana Zain Nabi Khan ¹ and Muhammad Ashraf ^{4,5}

¹ Centre of Excellence in Water Resources Engineering, University of Engineering and Technology, Lahore 54890, Pakistan; dr.ijaz@uet.edu.pk (I.A.); waseem.jatoi@cewre.edu.pk (M.W.); znk@cewre.edu.pk (R.Z.N.K.)

² School of Climate Change and Adaptation, University of Prince Edward Island, 550 University Ave., Charlottetown, PE C1A 4P3, Canada; faziz@upei.ca

³ Department of Irrigation and Drainage, University of Agriculture, Faisalabad 38000, Pakistan; muhammad.zaman@uaf.edu.pk

⁴ Department of Agricultural Engineering, Khwaja Fareed University of Engineering and Information Technology, Rahim Yar Khan 64200, Pakistan; dr.ashraf@kfueit.edu.pk

⁵ Commonwealth Scientific and Industrial Research, Organization Land and Water, Canberra 2601, Australia

* Correspondence: xxwang@upei.ca



Citation: Ahmad, I.; Wang, X.; Waseem, M.; Zaman, M.; Aziz, F.; Khan, R.Z.N.; Ashraf, M. Flood Management, Characterization and Vulnerability Analysis Using an Integrated RS-GIS and 2D Hydrodynamic Modelling Approach: The Case of Deg Nullah, Pakistan. *Remote Sens.* **2022**, *14*, 2138. <https://doi.org/10.3390/rs14092138>

Academic Editor: Luca Brocca

Received: 24 February 2022

Accepted: 27 April 2022

Published: 29 April 2022

Publisher's Note: MDPI stays neutral with regard to jurisdictional claims in published maps and institutional affiliations.

Abstract: One-dimensional (1D) hydraulic models have been extensively used to conduct flood simulations for investigating flood depth and extent maps. However, the 1D models cannot simulate many other flood characteristics, such as flood velocity, duration, arrival time and recession time when the flow is not restricted within the channel. These flood characteristics cannot be disregarded as they play an important role in developing flood mitigation and evacuation strategies. This study formulates a two-dimensional (2D) hydrodynamic model combined with remote sensing (RS) and geographic information system (GIS) approach to generate additional flood characteristic maps that cannot be produced with 1D models. The model was applied to a transboundary river of Deg Nullah in Pakistan to simulate an extreme flood event experience in 2014. The flood extent images from the moderate resolution imaging spectroradiometer (MODIS) and observed flood extents were used to evaluate the model performance. Moreover, an entropy distance-based approach was proposed to facilitate the integrated multivariate flood vulnerability classification. The simulated 2D flood modeling results showed a good agreement with the flood extents registered by MODIS and the observed ones. The northwest parts of Deg Nullah near Seowal, Dullam Kahalwan and Zafarwal were the most vulnerable areas due to high flood depths and prolonged flooding duration. Whereas high flood velocities, short flood arrival time, prolonged flood duration and recession times were observed in the upper reach of Deg Nullah thereby making it the most susceptible, critical and vulnerable region to flooding events.

Keywords: HEC-RAS 2D model; flood characterization; flood vulnerability; flood hazard maps; Deg Nullah



Copyright: © 2022 by the authors. Licensee MDPI, Basel, Switzerland. This article is an open access article distributed under the terms and conditions of the Creative Commons Attribution (CC BY) license (<https://creativecommons.org/licenses/by/4.0/>).

1. Introduction

Floods are considered the most devastating hazard all over the world. Floods claim more loss of life than any other hydrometeorological disasters [1], and negatively affect the socioeconomic development of many countries [2]. Moreover, the frequency and intensity of these flood events are increasing in many regions around the world, making it a problem of major concern in the sustainable development of countries vulnerable to flooding events [3]. The main reason behind these unprecedented flood events is the rise in temperature and precipitation since the 1950s due to anthropogenic activities and increased

rates of greenhouse gas emission [4]. Moreover, the increase in population growth rate and urbanization led to increased impervious areas and increased runoff due to the reduced infiltration [5]. Recent flood events are becoming more frequent and severe in Pakistan due to the population growth and increasing anthropogenic activities in the floodplains [6].

Pakistan faces almost one major flood event every three years [7] and drought-like conditions every six years [8], which is one of the main challenges to the country's sustainable economic development. Pakistan faced the worst flood event of its history in 2010 [9]. Scientists from the World Climate Research Program and World Meteorological Organization (WMO) stated that climate change was one of the main reasons behind this unprecedented sequence of weather events in Pakistan [10]. Moreover, a United Nations (UN) based scientific body stated that the hot extremes, heat waves and heavy precipitation events are expected to be more frequent and intense in the future in this country [11]. WMO also qualified the assessments that the flood event of 2010 fit the sequence as predicted by climate experts and stated that these events match the projections of more frequent and intense climatic events due to global warming [12].

In recent years, remote sensing (RS) and geographic information systems (GIS) played an important role in presenting and validating the flood risk and hazard mapping results [13,14]. RS and GIS are considered effective geospatial tools assisting in preparing the flood characteristic maps and their impacts on the environmental, social and economic aspects [15]. These geospatial tools have been extensively used to map the results of simulation models of past flood events such as flood inundation extents, flood levels and to identify the critical facilities at risk [16,17]. These tools also support developing the flood forecasting and early warning systems in flood-prone areas, which are helpful in flood hazard management and preparedness planning [18,19]. RS is an important tool in acquiring the data required to formulate and validate the flood model result, flood risk assessment and to identify the infrastructure at risk (e.g., health and education facilities, transportation infrastructure, urban and commercial areas, etc.). Whereas, use of GIS helps in developing automated flood models and flood risk investigations (identification of urban areas, settlements and agricultural lands to different stages of floods), to generate flood inundation maps and to conduct other statistical analyses that may be useful in developing the flood disaster management strategies at various levels of flood events [20]. For instance, the analytical hierarchy process (AHP) method and a geographical information system (GIS) were utilized to create the flood hazard assessment map in the burned and urban areas of central Greece [21].

Assessment of flood risk and management practices is important in identifying the flood hazards, flood-prone areas and future mitigation strategies [22]. Understanding the characteristics of floods is essential in developing flood management action plans and analyzing the impact of various proposed management measures. In situ observations of flood events are the simplest ways to interpret the flood risk [23]. However, in situ observations of the floods are not available in many cases in developing countries. Moreover, flood analysis based on these observations is limited to specific flood events. Therefore, one of the other ways to conduct flood risk modeling studies is to use the RS data [24,25]. However, flood events usually occur under cloudy conditions, limiting the application of remotely sensed data in the visible and infrared spectrum due to visibility issues [26]. Therefore, these observation maps cannot be used directly to predict future flood events and to analyze the efficacy of various structural measures in developing flood mitigation strategies. The numerical models are considered more suitable for the simulation and prediction of flood events. Moreover, in many previous studies, numerical models have been efficiently applied to simulate flood events and investigate the flood hazards to develop management strategies [27–29].

Both one-dimensional (1D) and two-dimensional (2D) numerical hydrodynamic models combined with RS and GIS approaches have been extensively used in numerous studies for simulating flood events and risk assessment [4,25,30]. Although 1D flood models can be used for simulating the water levels and discharges when the flow is restricted within the channels [31,32], these models present many limitations when applied for simulating the overflow conditions. Moreover, methodologies used by 1D flood models are limited to generating flood hazard and depth maps. Flood depth maps are considered the primary input in evaluating flood impacts. However, additional flood characteristic maps, i.e., flood velocities, flood arrival times, flood duration and flood recession times, cannot be disregarded as they play an important role in the detailed design and analysis stages of flood mitigation studies [20]. For instance, high flood velocities with a longer flood duration can damage the flood mitigation structures and result in erosion and water pollution, which may cause environmental degradation, economic and life losses [33]. Awadallah et al. [34] used the LiDAR datasets in the HEC-RAS 2D model for comparing the flood inundations maps using the bathymetric and topographic terrain models in Norway. Therefore, the use of 2D models becomes indispensable to address the above-mentioned issues.

In previous studies, several researchers have used the 2D hydrodynamic models to assess flood risks and develop flood mitigation strategies. For instance, Santillan et al. [20] applied an integrated RS, GIS and 2D hydrodynamic modeling approach to generate flood characteristic maps, i.e., flood velocity, arrival time, flood duration and recession time, for improved flood disaster management in the Philippines. Quiroga et al. [31] used a 2D numerical model to perform the unsteady flow analysis and compared the model results with the satellite imagery in the floodplains of Bolivian Amazonia, Brazil. In another study, an integrated 1D/2D hydrodynamic model was applied to generate the flood hazard maps and velocities in the floodplains of the Musi river basin of Indonesia [35]. Bhandari et al. [4] employed the 2D hydrodynamic modeling approach to perform the unsteady flow analysis and flood inundation mapping to outline the flood-prone areas in the lower reaches of the Brazos river basin, USA. Elkhrachy [36] used the remote sensing images as independent variables in the HEC-RAS 2D simulation model to estimate the post-flash flood event depths of 24–26 April 2018 in New Cairo, Egypt. Moreover, 2D hydrodynamic modeling approaches combined with RS and GIS have been applied since the release of the HEC-RAS 2D model in different regions of the world to investigate the flood events and to develop mitigation strategies [37–42].

Even with the extensive flood simulations using the hydrodynamic models to generate the flood hazard and depth maps, it is almost impossible for the decision-makers to develop flood mitigation and management strategies without analyzing the vulnerability of different elements at risk in the floodplains [43]. The concept of vulnerability has changed drastically in various disaster management studies based on their objectives. Consequently, several attempts were made to define the term vulnerability. For instance, Cutter [44] defined vulnerability as a hazard that includes natural risks and human response to these risks. However, Mitchell [45] stated that vulnerability is the degree of loss to a given element at risk (or set of elements) resulting from a given hazard at a given severity level. Moreover, Merz et al. [46] and Salami et al. [47] stated that it is a function of the vulnerability definition to elements at risk, exposure and susceptibility. The vulnerability of different elements (e.g., road networks, bridges, urban areas/settlements, etc.) at risk in the floodplains largely depends on water depth, flood velocities and duration of flooding [48]. Santillan et al. [20] categorized the levels of the flood hazard based on maximum depths into three classes, i.e., low (<0.5 m depth), medium (0.5–1.5 m depth) and high (>1.5 m depth) for the residential buildings. However, in most of the previous studies, flood extents and water depth were considered; whereas the flood variables such as flow velocities, flood duration and recession times were discussed only in a few studies [31,49]. For instance, Balijepalli and Oppong [50] suggested that the flood velocities of less than 2–3 m/s do not affect the physical infrastructure (e.g., road networks, bridges and urban areas/settlements) in floodplains. However, to the best of the author's knowledge, no study has been conducted

that performs the multivariate flood vulnerability analysis by using a 2D hydrodynamic flood modeling approach. Moreover, no flood research has been carried out by using an integrated RS-GIS and 2D hydrodynamic modeling approach together with vulnerability analysis in Pakistan to generate flood characteristics other than depth for developing flood management strategies.

Therefore, this study aims to simulate an extreme flood event with a return period of 200 years in Deg Nullah of Pakistan using an integrated RS-GIS and a 2D hydrodynamic modeling approach to generate the additional flood characteristic maps, i.e., flood velocities, arrival times, duration and flood recession times. The study area is subjected to frequent floods and result in disruption of socio-economic activities. Moreover, flood vulnerability analysis was performed to investigate the sensitivity of roads, railway tracks and urban areas/settlements at risk to different flood variables such as flood depths, velocities, arrival times, duration and recession times in the study area. Therefore, it is believed that the results of the present study would help develop improved flood management strategies.

2. Study Area

Deg Nullah, a natural drain in Rachna Doab of Punjab province, was analyzed to simulate the 2014 major flood event. Two streams, Divak and Basenter join together in the Indian Administered Kashmir to form Deg Nullah before diverting into Pakistan near Lehri check post, located in the northeast of Narowal district. Deg Nullah is a straight twisted channel with wide and shallow cross-sections and uneven slopes. Flows of Deg Nullah often overspill during the monsoon season as its banks are not high enough to pass the large discharges. There is a reach of 75 km from Kingra-more to the Bambanwala-Ravi-Bedian (BRB) canal, as shown in Figure 1. Deg Nullah mostly remains dry, but carries a large volume of flows during monsoon season. The catchment of Deg Nullah receives most of the precipitation in summer (July to September) [51]. This heavy precipitation resulted from the combined effects of the monsoon precipitation regime from the Arabian Sea and Bay of Bengal, making it a meteorological complex region. Precipitation over the catchment of Deg Nullah causes high flow peaks during the monsoon season and the deteriorated condition of shallow banks intensifies the flooding problem and affects the road networks, urban areas, settlements, agricultural lands, etc.

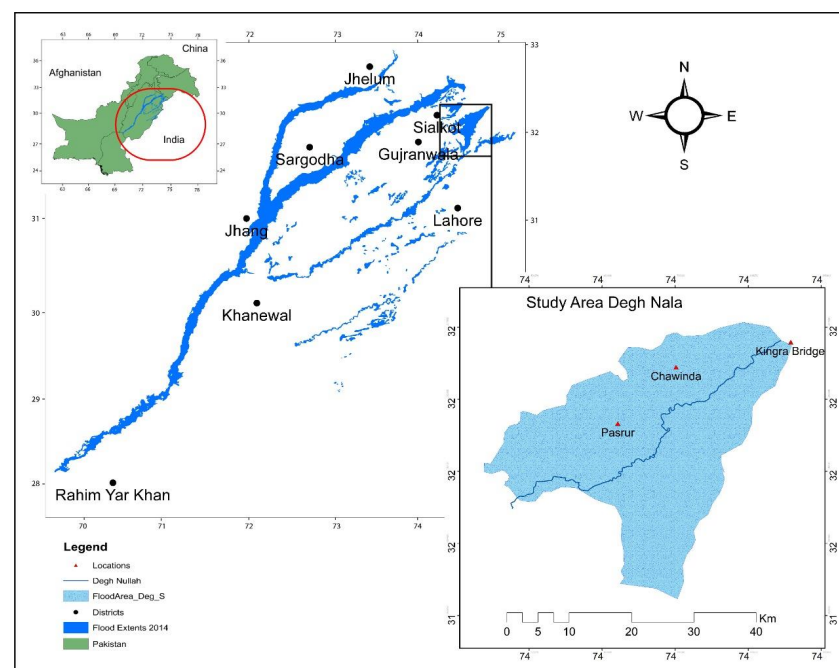


Figure 1. Location of the study area.

In 2014, Deg Nullah experienced one of the worst flood events of its history and caused severe damage to its surrounding areas. A peak flood of 2050 m³/s with a return level of 200 years was observed in Deg Nullah on 6 September 2014 [52]. Therefore, water overflowed from the banks of the Nullah and caused submergence in Zafarwal city, Qila Ahmedabad town and 55 villages around Deg Nullah. This flood event caused the displacement of a vast population from urban areas/settlements, road networks were damaged due to submergence and negatively affected the standing crops over a large area. Moreover, more than 25 health centers and 104 government schools were submerged [53]. Residents of this area blamed the Deg Nullah authorities for not providing accurate information regarding the flood events. Therefore, accurate evaluations of the flood extents, depth, velocity, arrival and recession times are essential for developing improved flood management strategies in this region.

3. Materials and Methods

3.1. Numerical Model

This study used a 2D hydrodynamic model (HEC-RASv5) due to its various advantages over 1D models. For instance, 1D flood models are considered suitable when the flow is restricted within the channel. However, when the overflow conditions prevail, it limits the applicability of 1D flood models in simulating flood characteristics and defining the flood flow directions. It is not always realistic to define the flow paths or directions in the floodplains, e.g., in flat areas with large variations in water levels, 1D models do not provide any information regarding the velocity distribution when the water leaves the main channel to the floodplains. However, these limitations can be efficiently addressed by 2D hydrodynamic flood modeling. These flood models can simulate additional flood characteristics such as flood arrival times, flood velocities, flood duration and flood recession times [54]. Moreover, remotely sensed datasets have been extensively used with the HEC-RAS 2D model to simulate, validate and forecast flood events in different regions of the world [16,20,34,36].

Therefore, a 2D hydrodynamic model (HEC-RAS 2D) developed by the USACE, was used to simulate the selected flood events in the Deg Nullah catchment area. This model solved either the full 2D Saint-Venant equations or 2D diffusive equation as given below:

$$\frac{\partial \xi}{\partial t} + \frac{\partial p}{\partial x} + \frac{\partial q}{\partial y} = 0 \quad (1)$$

$$\frac{\partial p}{\partial t} + \frac{\partial}{\partial x} \left(\frac{p^2}{h} \right) + \frac{\partial}{\partial y} \left(\frac{pq}{h} \right) = - \frac{n^2 pg \sqrt{p^2 + q^2}}{h^2} - gh \frac{\partial \xi}{\partial x} + pf + \frac{\partial}{\rho \partial x} (h\tau_{xx}) + \frac{\partial}{\rho \partial y} (h\tau_{yy}) \quad (2)$$

$$\frac{\partial q}{\partial t} + \frac{\partial}{\partial y} \left(\frac{q^2}{h} \right) + \frac{\partial}{\partial x} \left(\frac{pq}{h} \right) = - \frac{n^2 pg \sqrt{p^2 + q^2}}{h^2} - gh \frac{\partial \xi}{\partial y} + qf + \frac{\partial}{\rho \partial y} (h\tau_{yy}) + \frac{\partial}{\rho \partial x} (h\tau_{xx}) \quad (3)$$

where ξ represents the surface elevation (m); p and q represent the specific flows in the x and y directions (m²/s); h depicts the depth of water (m); g is the acceleration due to gravity (m/s²); n is the Manning roughness coefficient, ρ represents the density of water (kg/m³); s_{xx} , s_{yy} and s_{xy} are the components of the effective shear stress and f is the Coriolis (s⁻¹) [31].

3.2. Overall View of the Research Approach

Numerical simulations of physical processes are considered efficient through an iterative development of the model. The accuracy of the numerical models depends upon the quality of the available data and hydrologic understanding of the problem being investigated. A brief description of the study approach being adopted to achieve the objectives is presented in the flowchart (Figure 2) and described in the subsequent paragraphs.

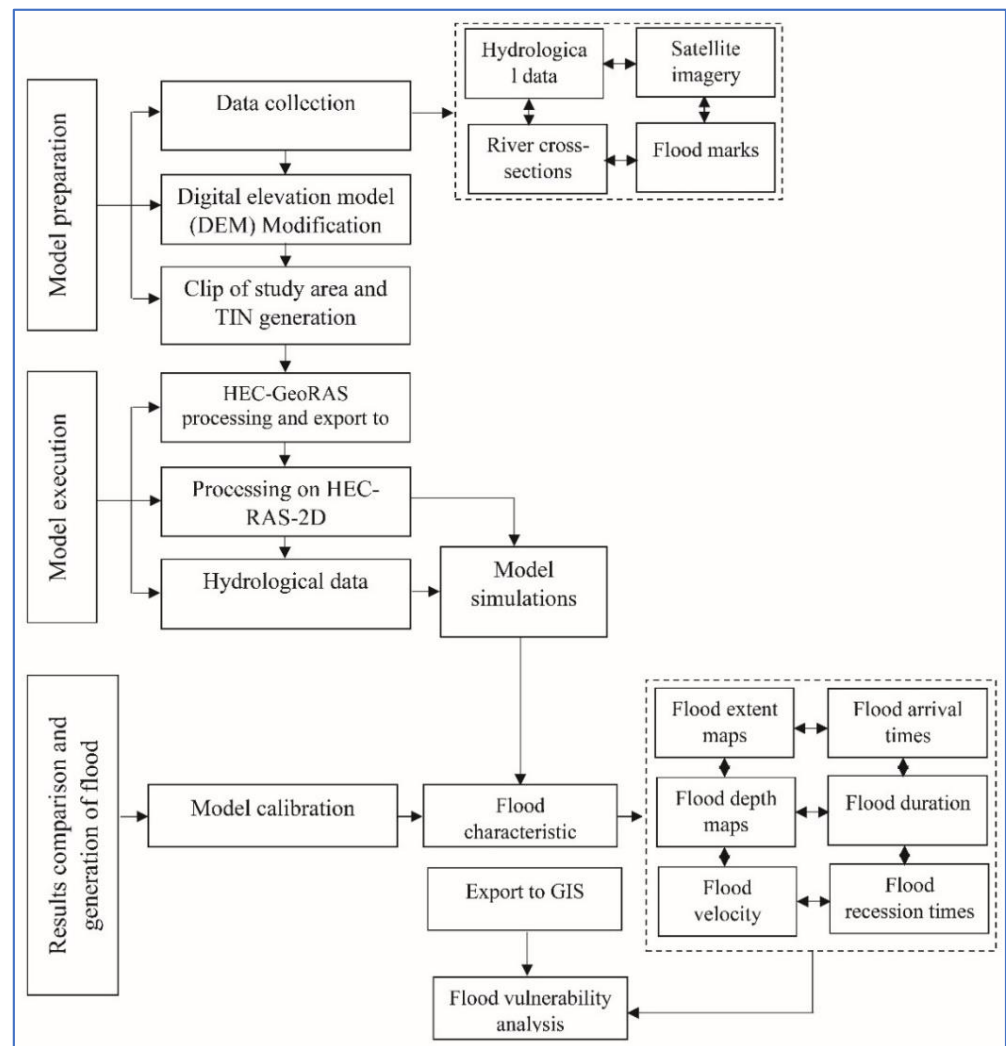


Figure 2. Overall summary of steps of methodology in the form of a flowchart.

The flow hydrographs of Deg Nullah at Kingra bridge station were collected from the Punjab Irrigation Department for the monsoon periods from 2014–2017 (Figure 3). The hydrograph data comprises an interval of one day. Among the collected hydrographs, the 2014 flood was the severest and was considered for flood analysis. The flow hydrograph of the Kingra bridge was used as the upstream boundary condition in the model.

The Shuttle Radar Topography Mission (SRTM) data are considered efficient in modeling the hydrological and hydraulic processes because of their free availability, homogeneity and consistency [55]. Therefore, the present study explores the hydrological modeling with the SRTM digital elevation model (DEM). The DEM with a resolution of 12.5×12.5 m was used. River cross-sections were considered the major input in both the 1D and 2D hydraulic modeling. The DEM was integrated with the observed cross-sections collected from the Punjab Irrigation Department at 53 locations across the Deg Nullah (Figure 4). The accuracy of the 2D hydrodynamic flood model, to analyze the water flow within the channel and floodplains (overflow conditions) was improved by integrating the DEM with the field observed cross-sections [20] and after that the study area was clipped from the DEM for further analysis. The DEM was then converted to a triangular irregular network (TIN) surface model whose surface does not deviate from the input raster. The DEM of the study area, along with the river cross-sections, is presented in Figure 4.

HEC-GeoRAS is a GIS extension designed to process geospatial data, allowing users to create an HEC-RAS import file containing geometric data. The results of the water

surface profiles can be interpreted to examine the flood depths and extents. In this study, preprocessing was conducted in HEC-GeoRAS to generate the model files. Afterward, the HEC-GeoRAS file consisting of geometric data was imported to HEC-RAS to perform the hydraulic computations.

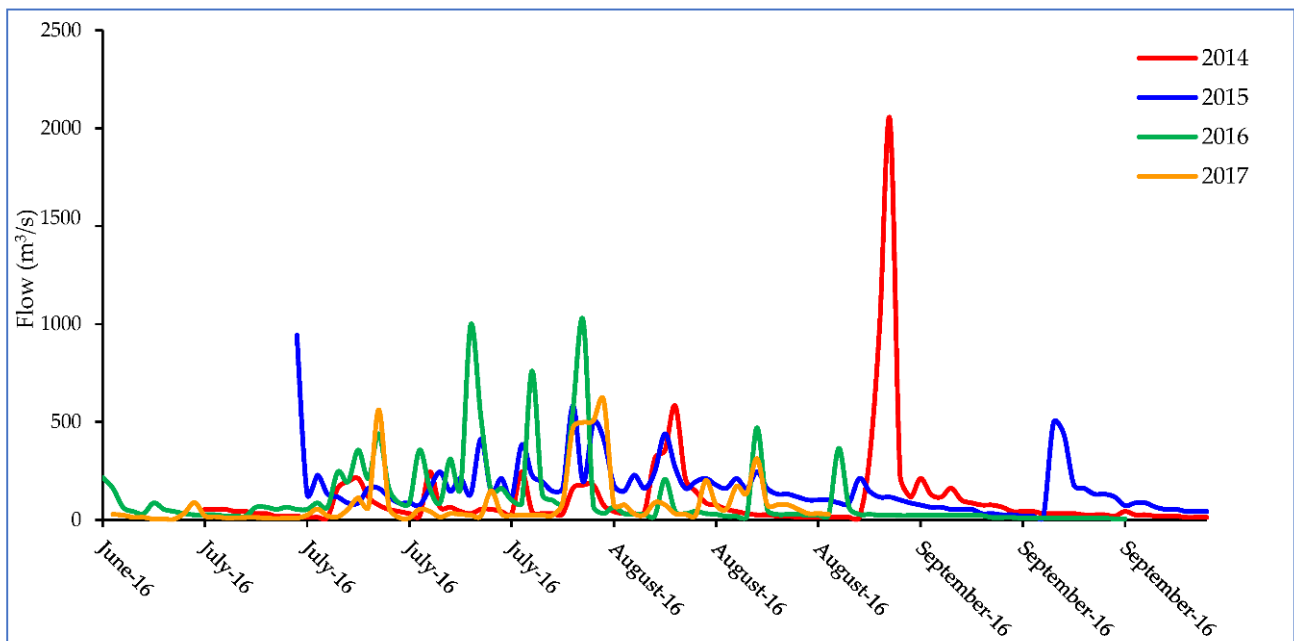


Figure 3. Observed flow hydrographs at Kingra bridge during monsoon periods of 2014–2017.

HEC-RAS model can either be used as an integrated 1D–2D model or as a fully 2D model to simulate the main rivers and floodplains, respectively. Although an integrated 1D–2D model might be faster compared to only the 2D modeling engine, it is necessary to define the connections of overflow locations between the 1D and 2D modules. In this study, a fully hydrodynamic 2D model was used, as the connections of overflow locations were unknown. The computational model domain (2D flow area) area was approximately 888 km². This area was discretized into 100 × 100 m size cells/grids. The model was run from 1 July 2014 to 7 October 2014 at a time step of 1 min, whereas output results were generated at 1-h intervals. Moreover, two types of boundary conditions were used in the 2D hydraulic model, i.e., inflow hydrograph as an upstream boundary condition at Kingra bridge of Deg Nullah and average riverbed slope was considered as the downstream boundary condition.

To compare the model-generated flood map with the observed flood extents (Table 1), the MODIS extent images were downloaded from <https://modis.gsfc.nasa.gov/data/> (accessed on 28 March 2019) for the monsoon period of 2014. In addition, two field visits were also conducted on 30 April 2019 and 15 May 2019 to collect the flood extents data at a few locations to verify the model simulated flood maps, ground-truthing of settlements and riverbed elevations by using GPS, and interviewing the locals and personnel from the irrigation department. A total of 32 imageries were downloaded from MODIS and a map showing the maximum extent was selected for the comparison of results.

Table 1. Observed flood extent locations.

Location No.	Longitude (E)	Latitude (N)
1	74°53′12.97″	32°18′39.65″
2	74°51′55.39″	32°14′15.79″
3	74°48′1.75″	32°22′22.1″

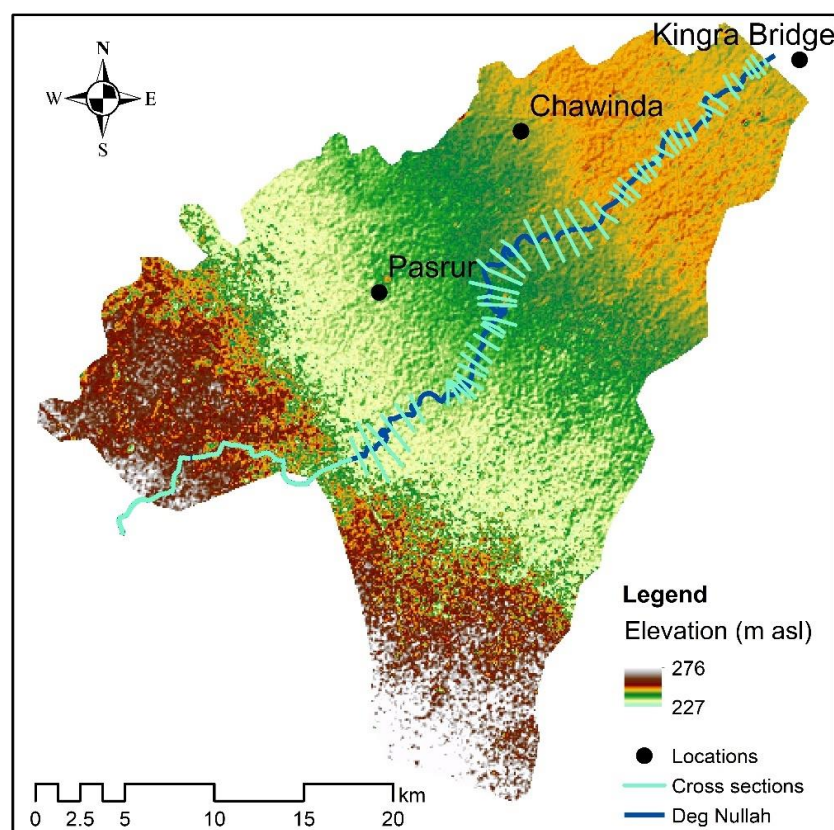


Figure 4. Observed river cross-sections, location of Deg Nullah and DEM of the study area.

3.3. Flood Vulnerability Analysis

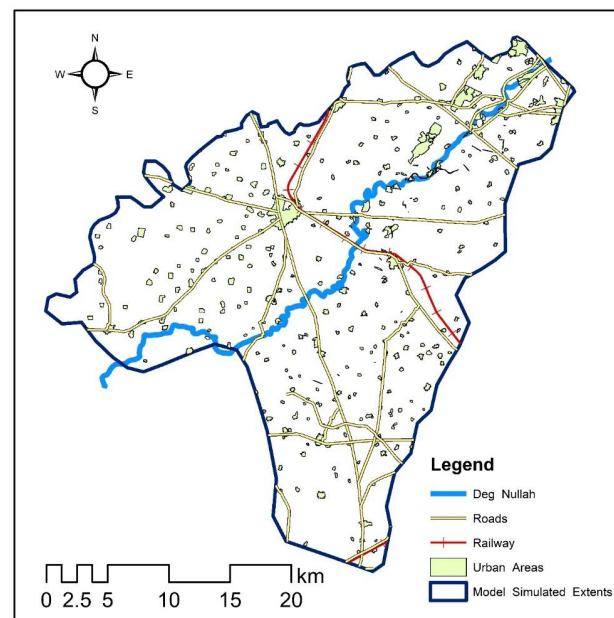
In this study, first, we digitized all the road networks, railway tracks and urban areas/settlements within the study area by using the satellite imageries (Google Earth Pro) and further verified their locations during the field visits, as shown in Figure 5. Secondly, various flood characteristic maps, i.e., flood depths, velocities, arrival times, duration and recession times, were superimposed on the digitized maps of the road networks and urban areas/settlements to investigate the flood risks at different locations in the study area. The details regarding the flood hazard classification based on flood depth, velocity, arrival time and duration are presented in Table 2 [31,50,56,57]. Moreover, the details regarding important urban areas (cities, villages, etc.) and road networks in the study area are presented in Table 3.

Table 2. Flood hazard classification based on maximum depth, velocity, duration and arrival time [26,44,51,52].

Hazard Level	Depth (m)	Velocity (m/s)	Duration (h)	Arrival Time (h)
Very low	<0.50	<1	<20	<14
Low	0.50–1.0	1–2	20–40	14–28
Medium	1.0–2.0	2–3.8	40–60	28–42
High	2.0–5.0	3.8–5.8	60–80	42–56
Extreme	>5.0	>5.8	>80	56–70

Table 3. Detaild of important locations (cities, villages, etc.) and road networks in the study area.

Sr. No.	Important Locations			Road Networks	
	ID on Map	Name of Location	ID on Map	Name of Road	Length of Road (km)
1	1	Kamalpur Bajwa	A	Pasrur road	29.0
2	2	Seowal	B	Chawinda road	28.5
3	3	Dullam Kahalwan	C	Gujranwala-Pasrur	19.1
4	4	Shahzada	D	Pasrur-Zafarwal	16.6
5	5	Kotli Haji Pur	E	Narowal road	20.3
6	6	Ahmad Abad	F	KalasaWala road	16.3
7	7	Dodha	G	Muridke road	12.1
8	8	Talwandi Bhindran	H	MirakPur road	16.2
9	9	Satrah Sandhuan	I	Nonar road	6.5
10	10	Pasrur	J	Daska road	10.2
11	11	Chawinda			
12	12	Zafarwal			

**Figure 5.** Digitized locations of the road networks and urban areas/settlements.

3.4. Multivariate Flood Vulnerability Classification

Once the standard values of the flood hazard level, i.e., very low, low, medium, high and extreme, of different flood variables, i.e., depth, velocity, arrival time and duration, were selected along with all the related information (Table 2), the entropy distance-based multivariate flood vulnerability classification was performed by using the following approach.

Let S_{ij} be the standard value of hazard level i of the j th flood variable, and P_{jk} is the value of the j th flood variable at location k .

Where $i = i$ th hazard level = 1, 2, ..., 5; $j = j$ th flood variable = 1, 2, ..., 4 and $k = k$ th location = 1, 2, ..., 383.

Normalization of S_{ij} and P_{jk} was performed to avoid any dimension-related issues by using Equations (4) and (5), respectively.

$$N_{ij} = \frac{\text{abs}(S_{ij})}{\sum_{i=1}^{n=5} \text{abs}(S_{ij})} \quad (4)$$

$$M_{jk} = \frac{\text{abs}(P_{jk})}{\sum_{k=1}^{n=383} \text{abs}(P_{jk})} \quad (5)$$

After that, difference of the normalized values and entropy-based weights were calculated by using the following equations

$$d_{jk} = M_{jk} - N_{ij} \quad (6)$$

$$w_j = \frac{e_j}{\sum_{j=1}^4 e_j} \quad (7)$$

in which

$$e_j = 1 - \left[\frac{-1}{\ln(N)} \sum_{k=1}^{n=383} M_{jk} \ln(M_{jk}) \right] \quad (8)$$

Finally, the entropy-based distance is calculated by using the following equation.

$$D_k = \sqrt{\sum_{k=1}^{383} w_j \cdot (d_{jk})^2} \quad (9)$$

where w_j is the entropy-based weight assigned to individual flood variables. D_k is the weighted Euclidean distance between the standard value of flood hazard level and the value obtained at different locations. A minimum value of the entropy-based distance of flood hazard level at a selected location represents the hazard level.

4. Results

4.1. Model Performance Evaluation

The performance of the HEC-RAS 2D model was evaluated by comparing the model simulated flood extents with the satellite image registered by MODIS on 6 September 2014. Moreover, two field visits were also conducted to identify the flood extents at three locations in the study area as shown in Figure 6 and summarized in Table 1. The image from 6 September 2014 was selected based on its maximum flood extents for calibration. Flood extents registered by MODIS and the simulated flood extents by the HEC-RASv5 model, along with the observed flood extents, are presented in Figure 6. It is clear from Figure 6 that the model simulated flood extents were consistent with the MODIS registered flood extents and the observed ones. The simulated flood extent was found 6% less compared to the flood extents obtained from the satellite image, which is considered acceptable due to the complexity of the system.

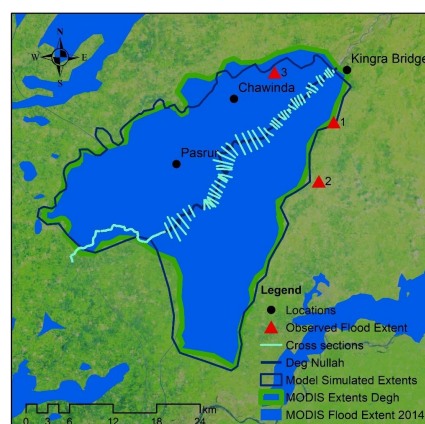


Figure 6. Comparison of model results with MODIS extents and observed flood marks.

4.2. Model Performance Evaluation

After successfully comparing the model results with the satellite imageries and observed flood extents, the HEC-RAS model was simulated to generate the flood characteristic maps of flood depths, velocities, arrival times, duration and recessions times. These flood characteristic maps are briefly discussed in the subsequent sections.

4.2.1. Maximum Flood Depths

The maximum flood depth map was generated using the 2D hydraulic model, as shown in Figure 7. This map was generated by considering the maximum depth of water in each cell during the simulation period regardless of the time when this depth was achieved. It was observed that the majority of the flooded areas north of the Deg Nullah have water depths of less than 1 m. Whereas the lower parts of the Deg Nullah have depths ranging from 0.5 m to 2 m. The most extreme flood depths were observed in the northeast part of the study area. However, these cells represent a small portion of the area compared to the rest of the wet cells. This map of flood depths can be useful in flood preparedness strategies and in developing evacuation plans when a flood of the same magnitude is expected to occur. This map can also help identify the areas required to be alerted or need emergency evacuation before future flood events. Moreover, the map of the maximum flood depths (Figure 7) can also be evaluated based on the various flood hazard levels. For instance, upstream reaches of the Deg Nullah experienced extreme flood hazards compared to the lower reaches as the flooded water overflowing from the channel spread over vast areas.

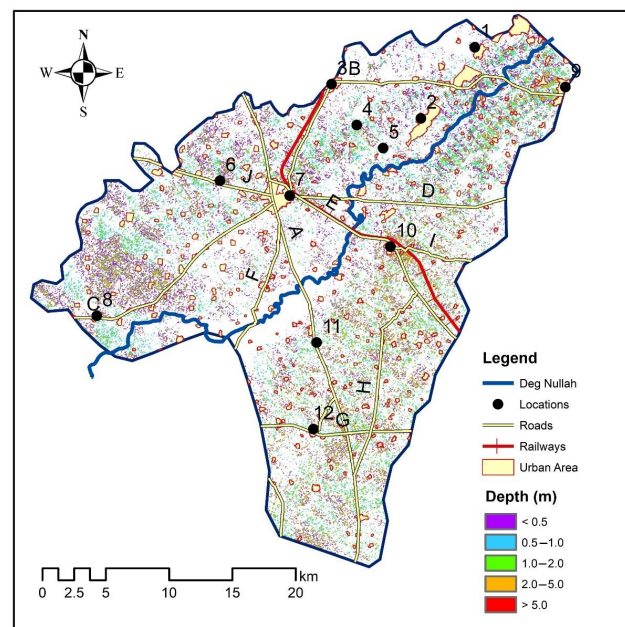


Figure 7. Map of the flood based on the maximum flood depths.

4.2.2. Maximum Flood Velocities

In addition to flood extent and depth maps, the HEC-RAS 2D model has the capability to generate velocity maps to depict the flood velocity at various locations in the study area as shown in Figure 8. The map of flood velocities would explain how fast the flood water will reach a particular location and thereby helps in developing flood mitigation strategies and evacuation planning. In most of the areas above the Deg Nullah, flood velocities vary between 0 to 1 m/s; whereas, in the western parts of the study area, the flood velocities were less than 0.5 m/s. Therefore, these areas are not expected to face severe flood risks due to flood velocities. However, flood velocities in the south of Deg Nullah vary from 0.5 to 1.5 m/s. At the upper reaches of Deg Nullah near Kingra bridge, flood velocities of more than 1.5 m/s were also observed. Such high flood velocities cause more water overflows from this point. Moreover, the areas with flood velocities of about 1 m/s or higher may pose additional hazards and evacuation will be more problematic due to the flash nature of flooding. These maps of flood velocities indicate the level of harm to which a community is exposed; therefore, they play an important role in developing flood risk management strategies.

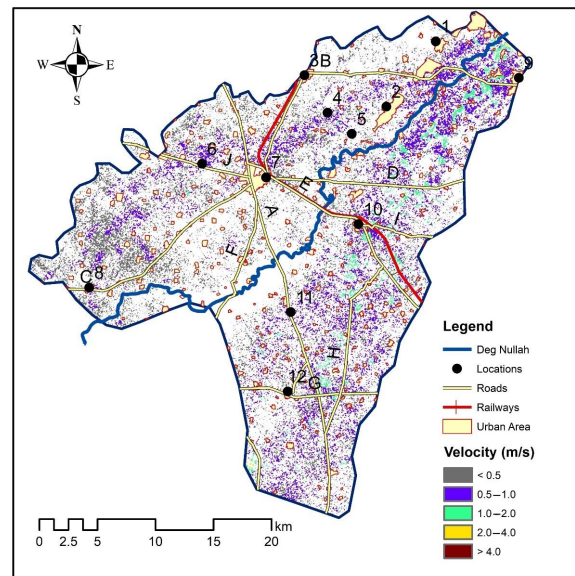


Figure 8. Map of the maximum flood velocities.

4.2.3. Flood Arrival Times

The maps of flood arrival times represent the model computed time from a specified simulation time when the water depth at a location reaches a specified inundation depth [54]. In this study, a flood arrival time map was generated in hours when a location is inundated at maximum depth (Figure 9). Most of the areas in the upper reaches of Deg Nullah achieved the maximum inundation depths within the first fourteen (14) hours. Whereas the lower reaches of the study area become flooded after 28 h from initiation of the flood event and so on. This implies that the areas in the upper reaches of the Deg Nullah are more vulnerable to floods and require a swifter evacuation response to flooding. These maps of flood arrival times are helpful in developing flood management and evacuation strategies.

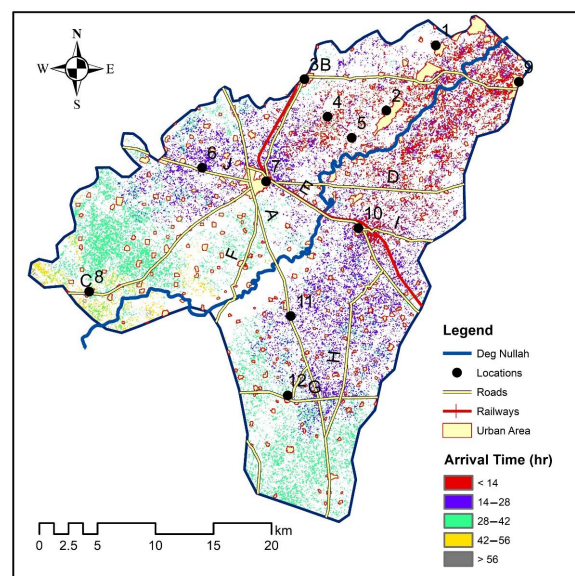


Figure 9. Map showing flood arrival times from the start of the simulation period at different locations of the study area.

4.2.4. Flood Duration

Figure 10 showed the flood duration map for the study. This map helps to understand the flood propagation in the areas that remain flooded for an extended duration. These

maps are considered very useful in estimating the time required for a flood-affected community to return to their respective areas and in assessing the flood damages to crops, road networks and other critical facilities located in the area. Figure 10 showed that most of the areas in the upper reaches remain flooded for more than 80 h. However, flood durations decreased in the areas of lower reaches of Deg Nullah.

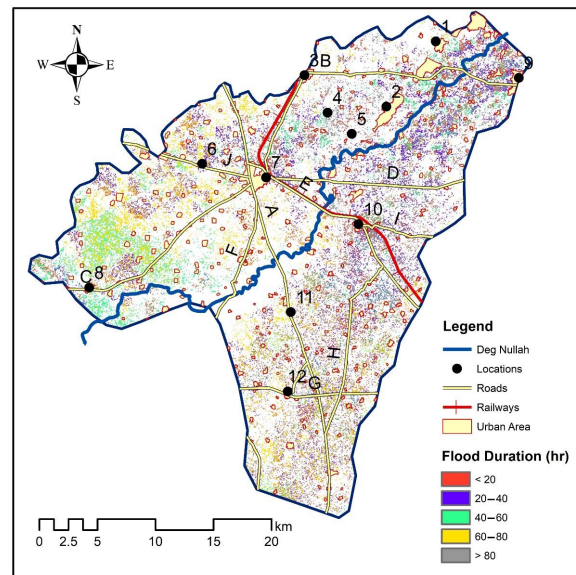


Figure 10. Map of flood duration at different locations of the study area.

4.2.5. Flood Recession Times

The map of flood recession times is presented in Figure 11. This map represents the number of hours that floodwater required to recede from different locations in the study area. The map of flood recession time generated showed that the flood-affected area required about 99 h to completely recede the inundation area generated due to the flood event of 2014. However, this duration decreased at locations far from the mainstream of Deg Nullah. This map has the same importance as flood duration in developing flood mitigation and management strategies.

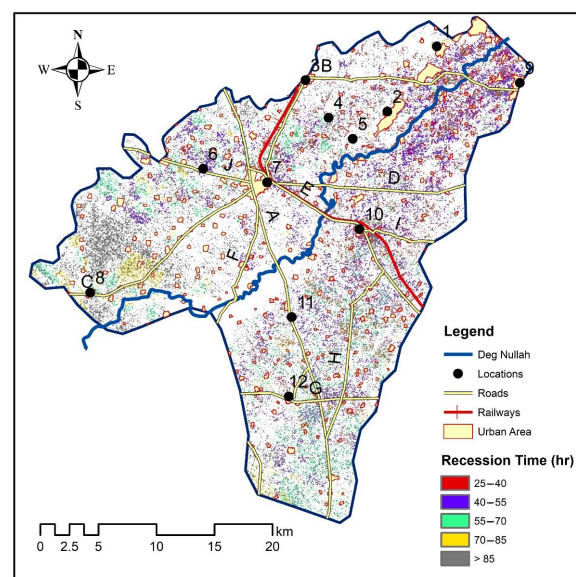


Figure 11. Map of flood recession times at different locations in the study area.

4.3. Flood Vulnerability Analysis

Physical infrastructure (e.g., road networks, railway tracks and urban areas/settlements) in the floodplains was considered to determine their vulnerability to flooding. The road networks and urban areas/settlements were digitized using the satellite imageries (Google Earth Pro) and later verified during the field visits. A total of 381 polygons of urban areas/settlements were marked in the study area. These polygons cover a total urban area/settlements of 47 km², which is about 6% of the entire study area. Whereas the total length of road networks in the study area was about 175 km connecting these urban areas/settlements and other major cities. The spatial flood characteristic maps, such as flood depths, velocities, arrival time, duration and recession time generated from the model for the flood event of September 2014, were superimposed on the maps of urban areas/settlements and road networks for vulnerability analysis. The results of the flood vulnerabilities to urban areas/settlements and road networks for various flood characteristic maps are presented in Figure 12. The flood vulnerability map is self-explanatory; however, flood hazard levels to maximum water depths and velocities are explained in the subsequent paragraph based on the water depths and velocities around the urban areas/settlements and road networks. Different flood hazard levels based on maximum depths are presented in Table 2.

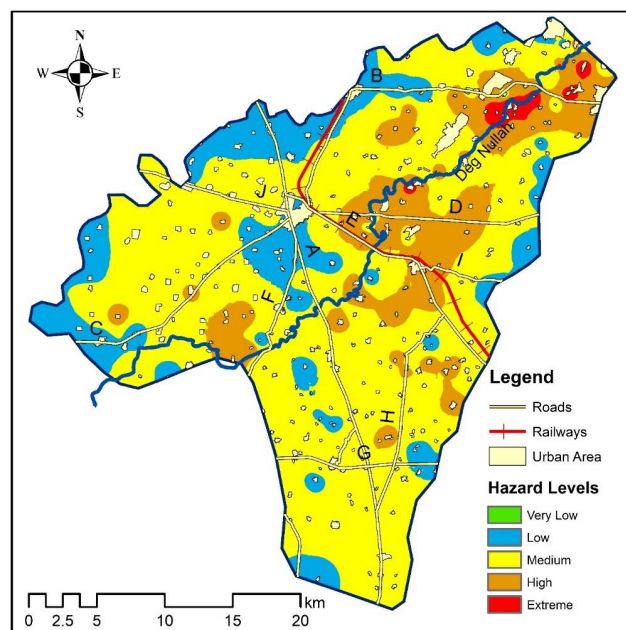


Figure 12. Multivariate flood hazard classification map along with the urban areas/settlements and road networks.

5. Discussion

Flooding events can significantly impact economic conditions and even threaten human life. These events are considered as the most disastrous among the hydro-meteorological hazards [58]. Hence, investigation of these events is highly important in developing mitigation strategies to reduce their negative impacts on human life and infrastructure. Flood simulation through hydraulic models has been extensively used for this purpose. The present research used the HEC-RAS 2D model for simulating an extreme flood event observed in a transboundary Deg Nullah which often experiences floods during the monsoon season and results in economic and human life loss. However, before the application of the model to generate flood characteristic maps, such as flood depth, velocity, arrival time, duration and recession time, the model simulated flood extents were compared with the extents registered by MODIS and later verified during the field visits. The model simulated flood showed good performance when compared with a satellite image of the

flood event [31]. The flood extent area simulated by the model was about 6% less than that as registered by MODIS extents. However, during the field visits, maximum flooding extents were verified by observations and discussions with locals at three different locations (Figure 6). Moreover, previous studies [27,59,60] confirmed the acceptability of the present study results in which the model simulated flood areas were found to be less compared to that of the satellite imageries. This reduction in the model simulated areas compared to satellite imageries may be due to the coarser DEM resolution [61] and due to the limitations of the HEC-RAS sub-grid configuration to produce a continuous inundation pattern that restricts the calculation of flood extent and the distribution of local water depth values [61]. Therefore, further studies may be carried out using the high-resolution DEM for improved model performance.

The maps of various flood characteristics such as flood depths, velocities, arrival times, duration and recession times were prepared to evaluate their distribution in the study area for an extreme flood event of $2050 \text{ m}^3/\text{s}$ [52]. The flood depth allows identifying areas exposed to different hazard levels. In most of the areas located in the northern part of Deg Nullah, the flood depths are less than 1 m whereas in its southern parts depth varies between 0.5–2 m, thereby posing low and low medium threats, respectively [56]. However, results have demonstrated that most of the settlements are constructed in the flood prone areas, which necessitates proactive planning and selection of the proper construction rules for the prevention and mitigation of the consequences of flood hazards. Over most of the flooded area, the water velocity was less than 0.1 m/s. However, water velocity in the south of Deg Nullah varies between 1–1.5 m/s, whereas at Kingra bridge it exceeds 1.5 m/s (Figure 8). The evacuation process may become difficult in areas with floodwater velocities of more than 1 m/s [57]. Flood arrival times at particular locations are one of the major variables along with velocity, depth, safe locations, etc., used to prepare the evacuation strategies [62]. The floodwater in the upper reaches of Deg Nullah attains the maximum depth within the first 14 h after the overflow condition, whereas in lower parts of the study area, it took more than 28 h and thereby, hazard levels are classified as low to medium [47]. The north part of the study area is the most exposed to the flood; it showed a larger flood extent, longer flood duration and deeper water depth. The flood that threatens the Seowal and Dullam-Kahalwan towns originates from the Kingra bridge, where the safe carrying capacity of the channel is only $280 \text{ m}^3/\text{s}$ [53]. The flood from the north gets close to Seowal hours after it begins to overflow, while it takes one day for the flood to reach the southern parts of the study area when the channel begins to overflow. Moreover, the flood in the north region is deeper than the flood in the south, the flood from the north begins to flood before the south. Therefore, flood hazard levels are higher in the northern region compared to the south and required efficient flood mitigation strategies. The study showed the applicability and the value of the 2D capabilities of the new HEC-RAS for flood studies.

Flood vulnerability of settlements and road networks to maximum water depths is presented in Figure 12. It is recorded that the vast majority of road networks are vulnerable to medium to high flood risks and may reduce the accessibility to certain parts of the areas or in the extreme, they may remain completely cut off from the rest until the affected links are revived [21]. Therefore, the vulnerability of road networks along with the urban areas and settlements to flood events was investigated by superimposing their digitized maps over the flood characteristic maps. The settlements in the upper reaches experienced medium to extreme flood hazard levels based on the water depths. However, these hazards decreased gradually as the flood water arrived in the lower reaches of Deg Nullah. Moreover, Balijepalli and Oppong [50] stated that the physical infrastructure (roads, bridges and buildings) is not subjected to severe damage for velocities below 2–3 m/s. In most areas, flood velocities are lower than 3 m/s and only a few locations in the upper reaches of Deg Nullah are experiencing flood velocities of more than 3 m/s as shown in Figure 8. However, the vulnerability of different infrastructures needs to be evaluated by considering the flood depths and velocities together. Therefore, multivariate flood vulnerability classification was performed to assess the combined effect of different flood variables (i.e., flood depth,

velocity, arrival time and duration and recession times) at various locations in the study area. Most of the study area lies within the medium hazard levels; however, upper and middle reaches near the channel pose high to extreme threats (Figure 12). Therefore, detailed studies related to the level of extreme events and the vulnerability of the exposed elements at risk (i.e., urban areas/settlements) will help propose the proper protection measures [63]. Moreover, the appropriate mitigation or hazard reduction approaches can be more effectively designed and applied. Furthermore, the awareness of the non-safe regions related to flood hazards might be helpful in emergency preparedness planning.

Therefore, scientists, engineers, stakeholders, planners and decision-makers may utilize the proposed approach in forthcoming spatial planning projects [64,65]. Additionally, the local authorities may use the produced map to guide the adoption of measures and strategies aiming toward flood hazard mitigation and post-fire management. The present study was limited to simulating the flood event of 2014 with return levels of 200 years. Further studies may be carried out for the floods of different return periods to develop flood mitigation strategies. Moreover, sediment and riverbed morphology may be included in the simulation for detailed investigation in future studies.

6. Conclusions

In this study, the extreme flood event of 6 September 2014 of Deg Nullah was simulated using a 2D HEC-RAS hydrodynamic model. The model simulated results showed a good agreement with flood extents registered by satellite images (MODIS) and observed flood extents. Moreover, flood characteristics, including depth, velocity, arrival time, duration and recession time, were generated by the HEC-RAS 2D model. Model simulated flood extents were found consistent with the flood extents registered by MODIS along with the field observed flood extents. Model simulated flood extent area was found 6% less than the flood extents obtained from the satellite image, which is considered acceptable.

The results of this study showed that the northwest parts of Deg Nullah near Seowal (ID-2), Dullam Kahalwan (ID-3) and Zafarwal (ID-12) were found most hazardous due to high flood depths and longer flood duration. Therefore, these areas are considered the most critical for evacuation. The flood velocities were found to be less than 1.5 m/s at most of the study area locations, thereby posing no serious threats due to the low velocity of the floodwater. However, in the upper reaches of Deg Nullah, floodwater velocities of greater than 2 m/s were observed. Moreover, flood duration in this region was also the longest among the rest of the areas. Therefore, high flood depths, flood velocities, longer flood duration and recession times and less flood arrival times make it the most critical and sensitive region to future flood events.

The present study analyzes the flood vulnerability of residential areas and road networks in the floodplains of Deg Nullah. Based on the hydrodynamic flood modeling results, it is noticeable that most of the residential areas and transportation infrastructure currently exists in medium to high flood risk zones and are likely to be exposed to future flood hazards of the same or more magnitudes. However, it was observed that the areas lying in the upper reaches of Deg Nullah were exposed to severe flood hazards due to high flood depths and velocities, faster flood arrival times, longer flood duration and recession times. Moreover, most of the urban areas/settlements in the middle and lower reaches of Deg Nullah were categorized in the range of low to medium hazard levels and the population may be considered safe inside their homes. Similarly, the road networks in the upper reaches were subjected to high flood depths and velocities which may influence the evacuation. The study showed that the HEC-RAS 2D model is an effective tool for studying and assessing the risk of flood events by coupling it with MODIS and other RS data in areas with little or no post-flood event information available. Future applications of the HEC-RAS 2D model with high-resolution DEM and other observed high floodwater marks may help analyze possible flood management strategies.

Author Contributions: Conceptualization, I.A. and R.Z.N.K.; data curation, M.W.; formal analysis, M.A.; funding acquisition, I.A.; investigation, M.W.; methodology, I.A., M.Z. and F.A.; project administration, I.A.; software, M.A., X.W., F.A. and R.Z.N.K.; supervision, X.W.; validation, M.Z.; visualization, M.Z.; writing—original draft, I.A. and F.A.; writing—review and editing, X.W. and M.A. All authors have read and agreed to the published version of the manuscript.

Funding: This research was funded funded by the Higher Education Commission of Pakistan (grant: SRGP-1593).

Data Availability Statement: Some or all data, models or code that support the findings of this study are available from the corresponding author upon reasonable request.

Acknowledgments: This research was funded funded by the Higher Education Commission of Pakistan (grant: SRGP-1593). The authors also thank the Punjab Irrigation Department for providing the data required for this research without any cost.

Conflicts of Interest: The authors declare that they have no conflict of interest in this work.

References

- Shadmehri, T.A.; Doulabian, S.; Ghasemi, T.E.; Calbimonte, G.H.; Alaghmand, S. Large-scale flood hazard assessment under climate change: A case study. *Ecol. Eng.* **2020**, *147*, 105765. [[CrossRef](#)]
- Smith, D.I. *Floods: Physical Processes and Human Impacts*; Smith, K., Ward, R., Eds.; John Wiley & Sons: Chichester, UK, 1999.
- Dewan, T.H. Societal impacts and vulnerability to floods in Bangladesh and Nepal. *Weather Clim. Extrem.* **2015**, *7*, 36–42. [[CrossRef](#)]
- Bhandari, M.; Nyaupane, N.; Mote, S.R.; Kalra, A.; Ahmad, S. 2D Unsteady Flow Routing and Flood Inundation Mapping for Lower Region of Brazos River Watershed. In Proceedings of the World Environmental and Water Resources Congress 2017, Sacramento, CA, USA, 21–25 May 2017; American Society of Civil Engineers: Reston, VA, USA, 2017; pp. 292–303.
- Thakur, B.; Parajuli, R.; Kalra, A.; Ahmad, S.; Gupta, R. Coupling HEC-RAS and HEC-HMS in Precipitation Runoff Modelling and Evaluating Flood Plain Inundation Map. In Proceedings of the World Environmental and Water Resources Congress 2017, Sacramento, CA, USA, 21–25 May 2017.
- FFC. *Annual Flood Report 2017*; Federal Flood Commission (FFC), Ministry of Water Resources, Government of Pakistan: Islamabad, Pakistan, 2017.
- Hashmi, H.N.; Siddiqui, Q.T.M.; Ghumman, A.R.; Kamal, M.A.; Mughal, H.R. A critical analysis of 2010 floods in Pakistan. *Afr. J. Agric. Res.* **2012**, *7*, 1054–1067.
- Ohlsson, L. Pakistan: IRIN Special Report on Water Crisis, Integrated Regional Information Network (IRIN). Available online: <http://www.padrigu.gu.se/EDCNews> (accessed on 31 May 2019).
- FFC. *Annual Flood Report 2010*; Federal Flood Commission (FFC), Ministry of Water & Power, Government of Pakistan: Islamabad, Pakistan, 2011.
- Coumou, D.; Rahmstorf, S. A decade of weather extremes. *Nat. Clim. Chang.* **2012**, *2*, 491–496. [[CrossRef](#)]
- IPCC, Climate Change. *The Physical Science Basis. Contribution of Working Group I to the Fourth Assessment Report of the Intergovernmental Panel on Climate Change*; Jansen, E., Overpeck, J., Briffa, K.R., Duplessy, J.C., Joos, F., Masson-Delmotte, V., Olago, D., Otto-Bliesner, B., Peltier, W.R., Rahmstorf, S., et al., Eds.; Cambridge University Press: Cambridge, UK, 2007.
- Gronewold, N. Is the Flooding in Pakistan a Climate Change Disaster? Available online: <http://www.scientificamerican.com/article/is-the-flooding-in-pakist/> (accessed on 31 May 2019).
- Sajjad, A.; Lu, J.; Chen, X.; Chisenga, C.; Saleem, N.; Hassan, H. Operational Monitoring and Damage Assessment of Riverine Flood-2014 in the Lower Chenab Plain, Punjab, Pakistan, Using Remote Sensing and GIS Techniques. *Remote Sens.* **2020**, *12*, 714. [[CrossRef](#)]
- Tayyab, M.; Zhang, J.; Hussain, M.; Ullah, S.; Liu, X.; Khan, S.N.; Baig, M.A.; Hassan, W.; Al-Shaibah, B. GIS-Based Urban Flood Resilience Assessment Using Urban Flood Resilience Model: A Case Study of Peshawar City, Khyber Pakhtunkhwa, Pakistan. *Remote Sens.* **2021**, *13*, 1864. [[CrossRef](#)]
- Sidek, L.M.; Chua, L.H.C.; Azizi, A.S.M.; Basri, H.; Jaafar, A.S.; Moon, W.C. Application of PCSWMM for the 1-D and 1-D-2-D Modeling of Urban Flooding in Damansara Catchment, Malaysia. *Appl. Sci.* **2021**, *11*, 9300. [[CrossRef](#)]
- Santillan, J.R.; Amora, A.M.; Makinano-Santillan, M.; Marqueso, J.T.; Cutamora, L.C.; Serviano, J.L.; Makinano, R.M. Assessing the impacts of flooding caused by extreme rainfall events through a combined geospatial and numerical modeling approach. *ISPRS—Int. Arch. Photogramm. Remote Sens. Spat. Inf. Sci.* **2016**, *XLI-B8*, 1271–1278. [[CrossRef](#)]
- Dasallas, L.; Lee, S.; Dasallas, L.; Lee, S. Topographical Analysis of the 2013 Typhoon Haiyan Storm Surge Flooding by Combining the JMA Storm Surge Model and the FLO-2D Flood Inundation Model. *Water* **2019**, *11*, 144. [[CrossRef](#)]
- Asare-Kyei, D.; Forkuor, G.; Venus, V. Modeling Flood Hazard Zones at the Sub-District Level with the Rational Model Integrated with GIS and Remote Sensing Approaches. *Water* **2015**, *7*, 3531–3564. [[CrossRef](#)]
- Al Baky, M.A.; Islam, M.; Paul, S. Flood Hazard, Vulnerability and Risk Assessment for Different Land Use Classes Using a Flow Model. *Earth Syst. Environ.* **2020**, *4*, 225–244. [[CrossRef](#)]

20. Santillan, J.R.; Marqueso, J.T.; Makinano-Santillan, M.; Serviano, J.L. Beyond Flood Hazard Maps: Detailed Flood Characterization with Remote Sensing, GIS and 2D Modelling. *ISPRS—Int. Arch. Photogramm. Remote Sens. Spat. Inf. Sci.* **2016**, *XLII-4/W1*, 315–323. [[CrossRef](#)]
21. Skilodimou, H.D.; Bathrellos, G.D.; Alexakis, D.E. Flood Hazard Assessment Mapping in Burned and Urban Areas. *Sustainability* **2021**, *13*, 4455. [[CrossRef](#)]
22. Su, X.; Shao, W.; Liu, J.; Jiang, Y.; Wang, K. Dynamic Assessment of the Impact of Flood Disaster on Economy and Population under Extreme Rainstorm Events. *Remote Sens.* **2021**, *13*, 3924. [[CrossRef](#)]
23. Hagen, E.; Lu, X.X. Let us create flood hazard maps for developing countries. *Nat. Hazards* **2011**, *58*, 841–843. [[CrossRef](#)]
24. Psomiadis, E.; Diakakis, M.; Soulis, K.X. Combining SAR and Optical Earth Observation with Hydraulic Simulation for Flood Mapping and Impact Assessment. *Remote Sens.* **2020**, *12*, 3980. [[CrossRef](#)]
25. Albu, L.M.; Enea, A.; Iosub, M.; Breaban, I.G. Dam Breach Size Comparison for Flood Simulations. A HEC-RAS Based, GIS Approach for Drăcșani Lake, Sitna River, Romania. *Water* **2020**, *12*, 1090. [[CrossRef](#)]
26. Tahsin, S.; Medeiros, S.C.; Hooshyar, M.; Singh, A. Optical Cloud Pixel Recovery via Machine Learning. *Remote Sens.* **2017**, *9*, 527. [[CrossRef](#)]
27. Di Baldassarre, G.; Schumann, G.; Bates, P.D. A technique for the calibration of hydraulic models using uncertain satellite observations of flood extent. *J. Hydrol.* **2009**, *367*, 276–282. [[CrossRef](#)]
28. Schober, B.; Hauer, C.; Habersack, H. A novel assessment of the role of Danube floodplains in flood hazard reduction (FEM method). *Nat. Hazards* **2015**, *75*, 33–50. [[CrossRef](#)]
29. Ruiz-Bellet, J.L.; Balasch, J.C.; Tuset, J.; Barriendos, M.; Mazon, J.; Pino, D. Historical, hydraulic, hydrological and meteorological reconstruction of 1874 Santa Tecla flash floods in Catalonia (NE Iberian Peninsula). *J. Hydrol.* **2015**, *524*, 279–295. [[CrossRef](#)]
30. Bhandari, S.; Jobe, A.; Thakur, B.; Kalra, A.; Ahmad, S. Flood Damage Reduction in Urban Areas with Use of Low Impact Development Designs. In Proceedings of the World Environmental and Water Resources Congress 2018, Minneapolis, MN, USA, 3–7 June 2018; American Society of Civil Engineers: Reston, VA, USA, 2018; pp. 52–61.
31. Quiroga, V.M.; Kure, S.; Udo, K.; Mano, A. Application of 2D numerical simulation for the analysis of the February 2014 Bolivian Amazonia flood: Application of the new HEC-RAS version 5. *RIBAGUA—Rev. Iberoam. Agua* **2016**, *3*, 25–33. [[CrossRef](#)]
32. Gilles, D.; Young, N.; Schroeder, H.; Piotrowski, J.; Chang, Y.-J.; Gilles, D.; Young, N.; Schroeder, H.; Piotrowski, J.; Chang, Y.-J. Inundation Mapping Initiatives of the Iowa Flood Center: Statewide Coverage and Detailed Urban Flooding Analysis. *Water* **2012**, *4*, 85–106. [[CrossRef](#)]
33. Ahmadisharaf, E.; Kalyanapu, A.J.; Chung, E.-S. Evaluating the Effects of Inundation Duration and Velocity on Selection of Flood Management Alternatives Using Multi-Criteria Decision Making. *Water Resour. Manag.* **2015**, *29*, 2543–2561. [[CrossRef](#)]
34. Awadallah, M.O.M.; Juárez, A.; Alfreksen, K. Comparison between Topographic and Bathymetric LiDAR Terrain Models in Flood Inundation Estimations. *Remote Sens.* **2022**, *14*, 227. [[CrossRef](#)]
35. Al Amin, M.B.; Sarino; Haki, H. Floodplain simulation for Musi River using integrated 1D/2D hydrodynamic model. *MATEC Web Conf.* **2017**, *101*, 05023. [[CrossRef](#)]
36. Elkhachy, I. Flash Flood Water Depth Estimation Using SAR Images, Digital Elevation Models, and Machine Learning Algorithms. *Remote Sens.* **2022**, *14*, 440. [[CrossRef](#)]
37. Liu, Z.; Merwade, V.; Jafarzadegan, K. Investigating the role of model structure and surface roughness in generating flood inundation extents using one- and two-dimensional hydraulic models. *J. Flood Risk Manag.* **2019**, *12*, e12347. [[CrossRef](#)]
38. Yalcin, E. Two-dimensional hydrodynamic modelling for urban flood risk assessment using unmanned aerial vehicle imagery: A case study of Kirsehir, Turkey. *J. Flood Risk Manag.* **2018**, *12*, e12499. [[CrossRef](#)]
39. Alivio, M.B.T.; Puno, G.R.; Talisay, B.A.M. Flood hazard zones using 2d hydrodynamic modeling and remote sensing approaches. *Glob. J. Environ. Sci. Manag.* **2019**, *5*, 1–16. [[CrossRef](#)]
40. Naeem, B.; Azmat, M.; Tao, H.; Ahmad, S.; Khattak, M.U.; Haider, S.; Ahmad, S.; Khero, Z.; Goodell, C.R. Flood Hazard Assessment for the Tori Levee Breach of the Indus River Basin, Pakistan. *Water* **2021**, *13*, 604. [[CrossRef](#)]
41. Papaioannou, G.; Varlas, G.; Terti, G.; Papadopoulos, A.; Loukas, A.; Panagopoulos, Y.; Dimitriou, E. Flood Inundation Mapping at Ungauged Basins Using Coupled Hydrometeorological–Hydraulic Modelling: The Catastrophic Case of the 2006 Flash Flood in Volos City, Greece. *Water* **2019**, *11*, 2328. [[CrossRef](#)]
42. Garcia, M.; Juan, A.; Bedient, P. Integrating Reservoir Operations and Flood Modeling with HEC-RAS 2D. *Water* **2020**, *12*, 2259. [[CrossRef](#)]
43. Tariq, M.A.U.R.; Farooq, R.; van de Giesen, N. A Critical Review of Flood Risk Management and the Selection of Suitable Measures. *Appl. Sci.* **2020**, *10*, 8752. [[CrossRef](#)]
44. Cutter, S. Vulnerability to Environmental Hazards. *Progress Human Geogr.* **1996**, *20*, 529–532. [[CrossRef](#)]
45. Mitchell, J. Urban disasters as indicators of global environmental change: Assessing functional varieties of vulnerability. In Proceedings of the Symposium on Disaster Reduction and Global Environmental Change, Federal Foreign Office, Berlin, Germany, 20–21 June 2002.
46. Merz, B.; Thielen, A.H.; Gocht, M. *Flood Risk Mapping at the Local Scale: Concepts and Challenges*; Springer: Dordrecht, The Netherlands, 2007; pp. 231–251.
47. Salami, R.O.; von Meding, J.K.; Giggins, H. Vulnerability of human settlements to flood risk in the core area of Ibadan metropolis, Nigeria. *Jamba* **2017**, *9*, 371. [[CrossRef](#)] [[PubMed](#)]

48. Pistrika, A.; Tsakiris, G.; Nalbantis, I. Flood Depth-Damage Functions for Built Environment. *Environ. Process.* **2014**, *1*, 553–572. [[CrossRef](#)]
49. Citeau, J.M. A New Flood Control Concept in the Oise Catchment Area: Definition and Assessment of Flood Compatible Agricultural Activities. In Proceedings of the FIG Working Week 2003, Paris, France, 13–17 April 2003.
50. Balijepalli, C.; Oppong, O. Measuring vulnerability of road network considering the extent of serviceability of critical road links in urban areas. *J. Transp. Geogr.* **2014**, *39*, 145–155. [[CrossRef](#)]
51. Hussain, M.S.; Lee, S. The regional and the seasonal variability of extreme precipitation trends in Pakistan. *Asia-Pacific J. Atmos. Sci.* **2013**, *49*, 421–441. [[CrossRef](#)]
52. Faisal, M.; Muzammil, M.; Azam, M.I.; Yaseen, M.; Abbas, T.; Nabi, G. Flood Hazard Mapping and Risk Zoning of the Nullah Deg, Pakistan Using Hydraulic Simulation Model (a Case Study). *Sci. Int.* **2015**, *27*, 6459–6464.
53. Faisal, M. *Assessment of Flood Inundation Using Hydraulic Simulation Model*; University of Engineering and Technology: Lahore, Pakistan, 2015.
54. USACE-HEC. *HEC RAS River Analysis System 2D Modelling User's Manual Version 5.0*; Hydrologic Engineering Center, United States Corps of Engineer: Davis, CA, USA, 2016.
55. Yang, L.; Meng, X.; Zhang, X. SRTM DEM and its application advances. *Int. J. Remote Sens.* **2011**, *32*, 3875–3896. [[CrossRef](#)]
56. Dang, N.M.; Babel, M.S.; Luong, H.T. Evaluation of food risk parameters in the Day River Flood Diversion Area, Red River Delta, Vietnam. *Nat. Hazards* **2011**, *56*, 169–194. [[CrossRef](#)]
57. Kreibich, H.; Piroth, K.; Seifert, I.; Maiwald, H.; Kunert, U.; Schwarz, J.; Merz, B.; Thielen, A.H. Is flow velocity a significant parameter in flood damage modelling? *Nat. Hazards Earth Syst. Sci.* **2009**, *9*, 1679–1692. [[CrossRef](#)]
58. Lea, D.; Yeonsu, K.; Hyunuk, A. Case Study of HEC-RAS 1D–2D Coupling Simulation: 2002 Baeksan Flood Event in Korea. *Water* **2019**, *11*, 2048. [[CrossRef](#)]
59. Horritt, M.S.; Di Baldassarre, G.; Bates, P.D.; Brath, A. Comparing the performance of a 2-D finite element and a 2-D finite volume model of floodplain inundation using airborne SAR imagery. *Hydrol. Process.* **2007**, *21*, 2745–2759. [[CrossRef](#)]
60. Horritt, M.S.; Bates, P.D. Evaluation of 1D and 2D numerical models for predicting river flood inundation. *J. Hydrol.* **2002**, *268*, 87–99. [[CrossRef](#)]
61. Shustikova, I.; Domeneghetti, A.; Neal, J.C.; Bates, P.; Castellarin, A. Comparing 2D capabilities of HEC-RAS and LISFLOOD-FP on complex topography. *Hydrol. Sci. J.* **2019**, *64*, 1769–1782. [[CrossRef](#)]
62. Musolino, G.; Ahmadian, R.; Xia, J. Enhancing pedestrian evacuation routes during flood events. *Nat. Hazards* **2022**, *2022*, 1–25. [[CrossRef](#)]
63. Bathrellos, G.D.; Skilodimou, H.D.; Chousianitis, K.; Youssef, A.M.; Pradhan, B. Suitability estimation for urban development using multi-hazard assessment map. *Sci. Total Environ.* **2017**, *575*, 119–134. [[CrossRef](#)]
64. Saunders, W.S.A.; Kilvington, M. Innovative land use planning for natural hazard risk reduction: A consequence-driven approach from New Zealand. *Int. J. Disaster Risk Reduct.* **2016**, *18*, 244–255. [[CrossRef](#)]
65. Panagopoulos, G.P.; Bathrellos, G.D.; Skilodimou, H.D.; Martsouka, F.A. Mapping Urban Water Demands Using Multi-Criteria Analysis and GIS. *Water Resour. Manag.* **2012**, *26*, 1347–1363. [[CrossRef](#)]